DOI: 10.21062/mft.2023.011 http://www.journalmt.com

Evaluation of Riveting Force Influence on the Quality of Riveted Joint of Aluminium Alloy EN AW - 6016

Josef Bradáč (0000-0003-4075-3616), Jiří Sobotka (0000-0002-6569-6593)
Department of Mechanical and Electrical Engineering, SKODA AUTO Vysoká škola o.p.s. Na Karmeli 1457, 291 01 Mladá Boleslav. Czech Republic. E-mail: josef.bradac@savs.cz, jiri.sobotka@savs.cz

Joining technologies are very important aspects of the production process in the automotive industry. This also applies to newly developed types of materials (e.g. ultra high-strength steels or aluminium alloys), where riveting or adhesive bonding technologies are used in addition to standard technologies such as welding. With regard to riveting technology, the correct setup of riveting parameters highly influences the resulting properties of the produced joints. Therefore, the aim of this article is to evaluate the effect of the riveting force on the final quality of the riveted joint in the case of aluminium alloy EN AW-6016 (thickness 2 mm). The evaluation of the riveted joint is carried out through selected tests. These include a shear test, a hardness test HV01 and a deformation analysis using non-contact optical scanning (ATOS III Triple Scan system).

Keywords: Riveting, Aluminium Alloy, Shear Test, Hardness, Digitalization

1 Introduction

The use of metals having low density (light metals) such as aluminium and magnesium has a long tradition e.g. in means of transport design. The main benefit of using these materials is the possibility to reduce the weight of the resulting parts. This is particularly very important nowadays when increasing demands are being placed on the efficiency of transport means and the reduction of CO_2 emissions [1]. This is particularly the case in the automotive industry, where unconventional materials and component technologies, such as parts with variable thicknesses (e.g. tailored blanks), are becoming increasingly popular [2]. Aluminium alloys are still an important and widely used material in the industry. In addition to weight reduction, their corrosion resistance and recyclability are also very beneficial. The desired properties of these alloys can be achieved both by the correct choice of alloying elements and by heat treatment [3, 4].

As far as aluminium alloy joining technologies are concerned, there are many joining methods. Each of the methods has certain advantages and disadvantages and this predetermines them to be used in specific applications. The most used methods include welding, soldering, riveting and bonding. Recently, combinations of these joining methods, such as welding and riveting [5] or a combination of bonding and riveting, have also become widely used. The major purpose of such modifications of joining technologies is to exploit the combined advantages of these technologies. It is thus possible to reduce the weight thanks to bonding [6] and increase the joint strength using riveting or welding. In the case of welding technology, both fusion and pressure welding methods can be applied. When welding aluminium alloys, the formation of a difficult-to-melt oxide layer on the surface of a material is particularly problematic and to fuse the material, relevant treatment must be performed. For larger sheet thicknesses, friction stir welding FSW can be a suitable method in certain applications [7]. For thin sheet metal, arc or laser welding and, in the automotive industry, resistance welding is mainly used. Here, in addition to the oxide layer, the high energy consumption during the process due to the physical properties of aluminium is also problematic [8]. For these reasons, mechanical joining techniques, such as riveting (especially e.g. self-piercing riveting technology), have been recently increasingly applied [9].

Riveting is an important method of joining materials with a very long history. It is mainly used in transport, i.e., in the shipping, aerospace and automotive industries [10, 11]. The advantage of riveting is the possibility to join materials with different physical and mechanical properties [12]. In addition to that, riveting does not produce harmful by-products that affect the environment and does not affect the thermal properties of used material. In terms of technology, there are several riveting methods. Self-piercing riveting is one of the important methods with the potential to be used for joining sheet metals in the automotive. To achieve the desired quality and dimensional accuracy of the parts, the correct choice of riveting parameters (especially the riveting force) is required [13]. This is because deformation in the rivet area can affect both the properties and the shape of the final part. Both experimental methods and numerical simulations are used to select the correct

riveting parameters [14]. This paper aims to show the effect of one of the main riveting parameters (riveting force) on the mechanical properties and dimensional accuracy of the aluminium alloy EN AW-6016. The thickness of the tested material was 2 mm. Moreover, an effort was also to select such tests, whose results can be quite easily used in the numerical simulations.

2 Basic mechanical properties of tested material and overview of performed experiments

First of all, the basic mechanical properties of the tested aluminium alloy EN AW-6016 were measured at room temperature. There were measured two basic strength properties (proof yield strength $R_{p0.2}$ and ultimate strength R_m) and two formability properties (uniform ductility A_g and total ductility A_{80mm}). Results, which are typical of alloy AW-6061, are summarized in Tab. 1. Static tensile test was carried out acc. to standard EN ISO 6892-1 with loading rate 1.5 mm·min^{-1} up to achieving proof yield strength and 15 mm·min^{-1} after that. Typical stress-strain curves for the tested aluminium alloy EN AW-6061 in dependence on the rolling direction are shown in Fig. 1.

Tab. 1 *Basic mechanical properties of the tested aluminium alloy EN AW-6016*

Aluminium alloy EN AW-6016	Basic mechanical properties			
	Strength properties		Formability properties	
	$R_{p0.2}$ [MPa]	R_m [MPa]	A_g [%]	A_{80mm} [%]
Rolling direction 0°	126.7	238.2	23.05	28.92
Rolling direction 45°	122.9	233.7	26.47	34.52
Rolling direction 90°	119.3	230.1	24.01	30.23

After the determination of basic mechanical properties, there were subsequently performed two material tests and one contact-less optical scanning. The major effort was to select tests, which can describe deformation from different points of view – an overview of their major purposes and required physical quantities is given in Tab. 2.

Tab. 2 *Overview of the performed experiments and their major purposes*

Test	Purpose of the measurement	Measured quantity	
Shear test	To determine max force during the shear test	Max. force	[N]
Hardness testing	To measure hardness distribution along the rivet (for further research also the strain distribution)	Vickers hardness	HV01
Contact-less optical scanning	To determine the influence of applied pressure on the final shape of riveted samples	Flatness	[mm]

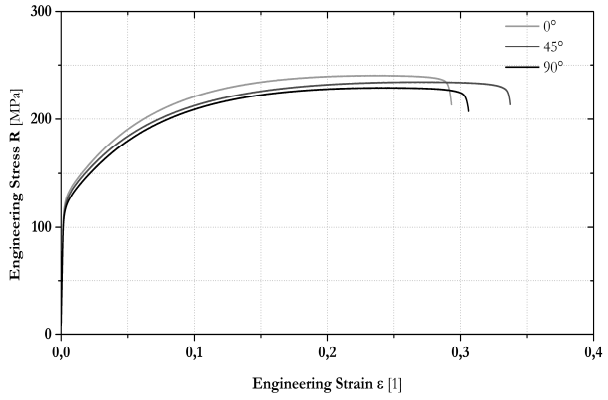

Fig. 1 *Engineering stress-strain curves for tested aluminium alloy EN AW-6061 regarding the rolling directions*

3 Preparation of the testing samples (riveting)

C-frame radial riveting machine from the German company TOX® PRESSOTECHNIK GmbH & Co. KG with a maximal riveting force of 158 kN (see Fig. 2), was used for the preparation of testing samples. There was used relevant die designed for aluminium alloys with a corresponding blank-holder and punch to carry out self-piercing riveting. Because of that, self-piercing rivets of diameter 5 mm, rivet head diameter 8 mm and length 5 mm were used. Such rivet diameter (5 mm) was used in consideration of the reality that a similar diameter is used at resistance spot welding in the automotive industry. So, for a better comparison

ISSN 1213–2489
e-ISSN 2787–9402

of results in further research. Major digital outputs were monitored during the self-piercing riveting.

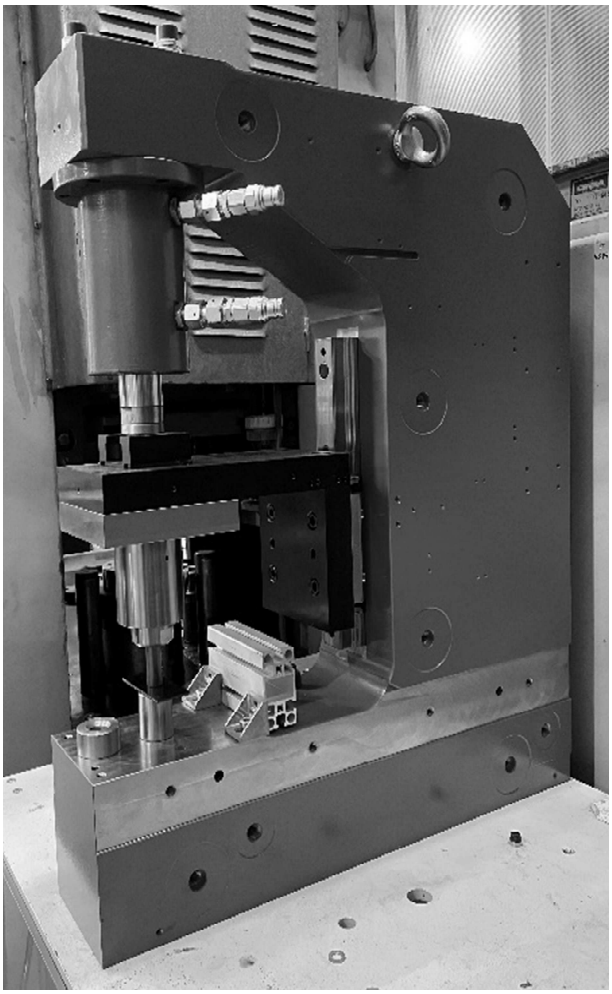

Fig. 2 *C-frame radial riveting machine*

Fig. 3 shows courses of applied pressures vs time during riveting. Regarding the tested aluminium alloy, three magnitudes of applied pressures were used: 6 MPa, 8 MPa and 10 MPa. These pressures correspond to the following riveting forces: 36 kN, 48 kN and 60 kN, respectively.

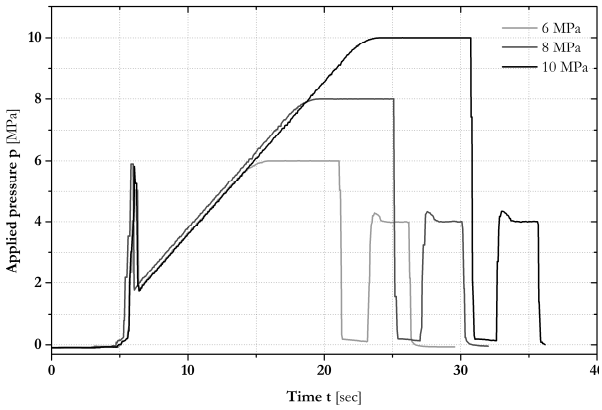

Fig. 3 *Applied pressure vs. time for all required maximal values of pressures (6, 8 and 10 MPa)*

4 Shear test

Another test that is especially important in the case of joining technologies, is a shear test. Testing samples for the shear test had dimensions as follows: width - 40 mm, length – 100 mm and finally, length of the overlap region was 30 mm. (see Fig. 4 – left). Rivet was subsequently applied right in the centre of the overlap region. Moreover, In Fig. 4 (right) are shown testing samples (applied pressure was 8 MPa) before and after implementation of the shear test, which was carried out on the testing device TIRAtest 2300.

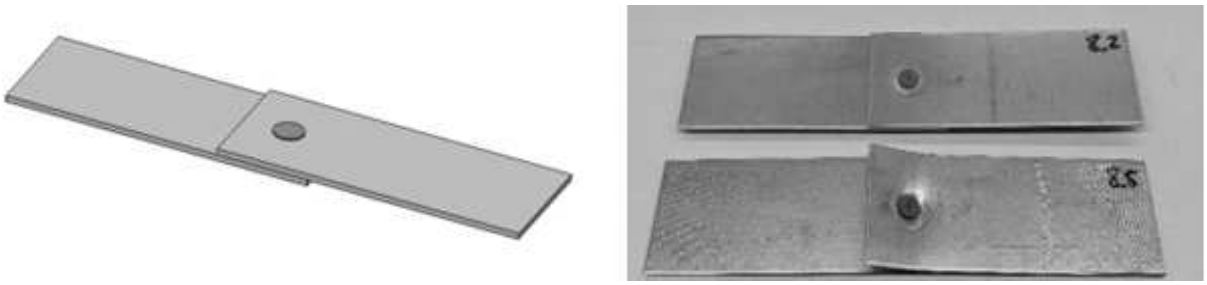

Fig. 4 *Designed shape of testing samples (left) and example of real samples before and after the shear test (right)*

The dependence of the force vs. time was primarily measured during the shear test. There was not used any extensometer in this case, because these shear tests were performed just to measure the maximum force for all monitored values of applied pressures (6, 8 and 10 MPa). Values of maximum forces, taken as arithmetic mean (x) and standard deviation (s) from the 10 samples for each applied pressure, are summarized in Tab. 3.

Tab. 3 *Maximal measured forces from the shear test*

Applied pressure p [MPa]		6 MPa	8 MPa	10 MPa
F_{MAX} [N]	x	**4784**	**5512**	**6037**
	s	104	202	25

indexed on http://www.webofscience.com and http://www.scopus.com

Fig. 5 gives a basic overview of the typically measured courses of relevant shear tests. Taking the result for the 6 MPa as the basic one (100 %), there is an increase by 15.22 % for 8 MPa and by 26.19 % for 10 MPa.

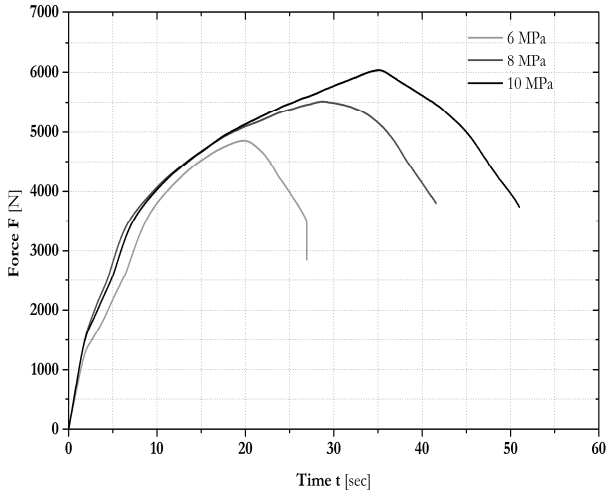

Fig. 5 *Force vs time from the shear test (examples for all tested values of applied pressures – 6, 8 and 10 MPa)*

5 Hardness testing

The next step in the series of experimental measurements to evaluate the influence of riveting force on the quality of riveted joints from aluminium alloy EN AW – 6016 was the hardness measurement. There were two major reasons to carry out such testing. The first one was just determining the hardness distribution along the riveted joint and the second one was the effort to know indirectly the magnitude of material hardening. Hardness testing was carried out on the hardness tester Qness Q30A and hardness HV01 was measured. In Fig. 6 (left) are shown images of the metallurgical scratch pattern for sample 6 MPa before and after hardness measurement. In Fig. 6 (right) are shown these results in more detail. It is clear, that the hardness of the basic material was ca. 85 HV01. Hardness values increase in the vicinity of a rivet and vary from 110 up to 120 HV01. The maximal hardness values of about 129 HV01 were determined right under the rivet in the area of maximal deformation of Al sheets.

As another step of this approach to determine the mechanical properties of riveted joints, there is a possibility to perform a common static tensile test and via the contact-less optical measurement of deformation to match relevant hardness and strain value. Although, there is just a uniaxial stress state during the static tensile test and in the vicinity of the riveted joint can be found various stress state types, it can provide some important information about the strain distribution. And just such results can be very useful e.g. for the numerical simulation of riveting.

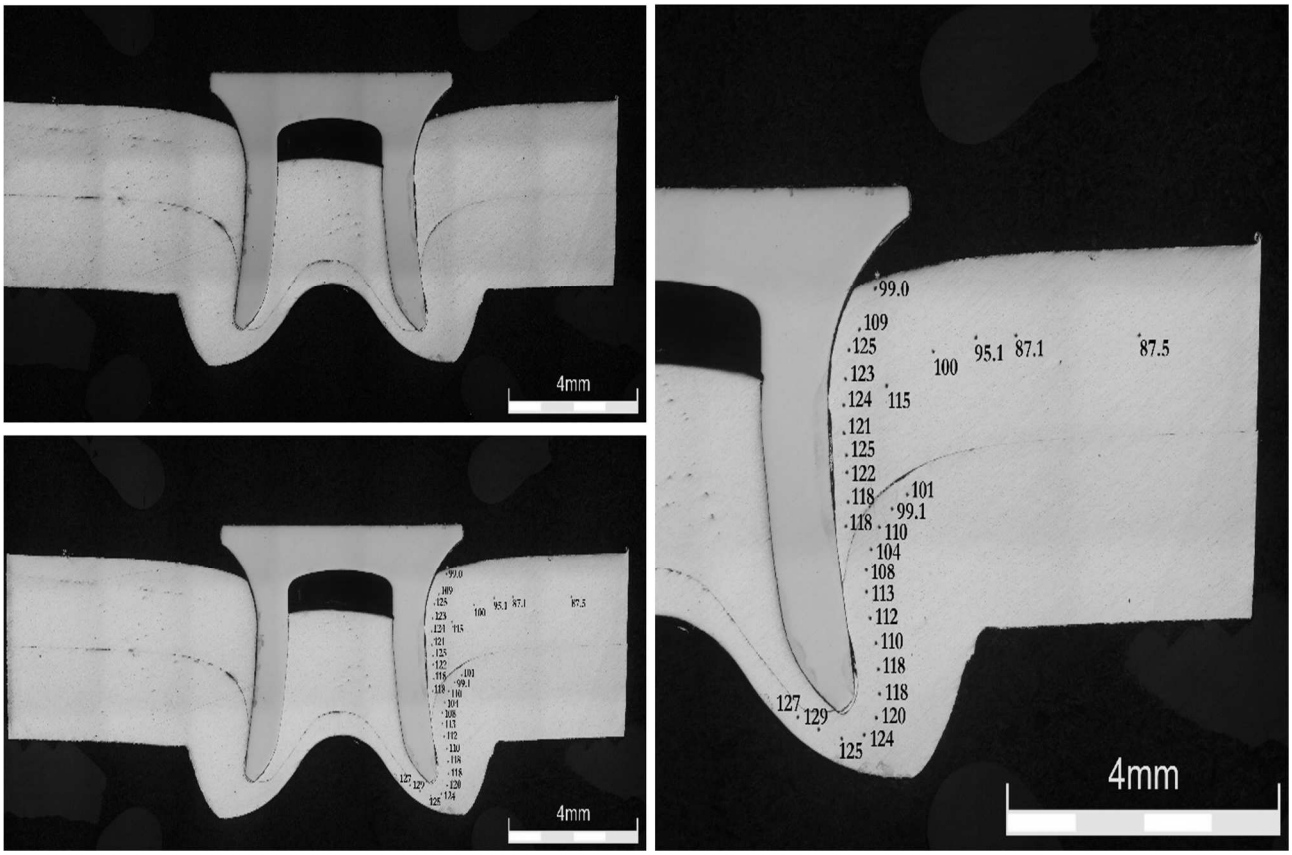

Fig. 6 *Hardness measurement for sample 6 MPa before and after hardness measurement (left) and detail (right)*

Fig. 7 shows hardness values for sample 8 MPa (left) and sample 10 MPa (right). The maximal hardness value was 134 HV01 for 8 MPa (higher by 3.9 %) and 138 HV01 for 10 MPa (higher by 7.0 %) – compared to 6 MPa.

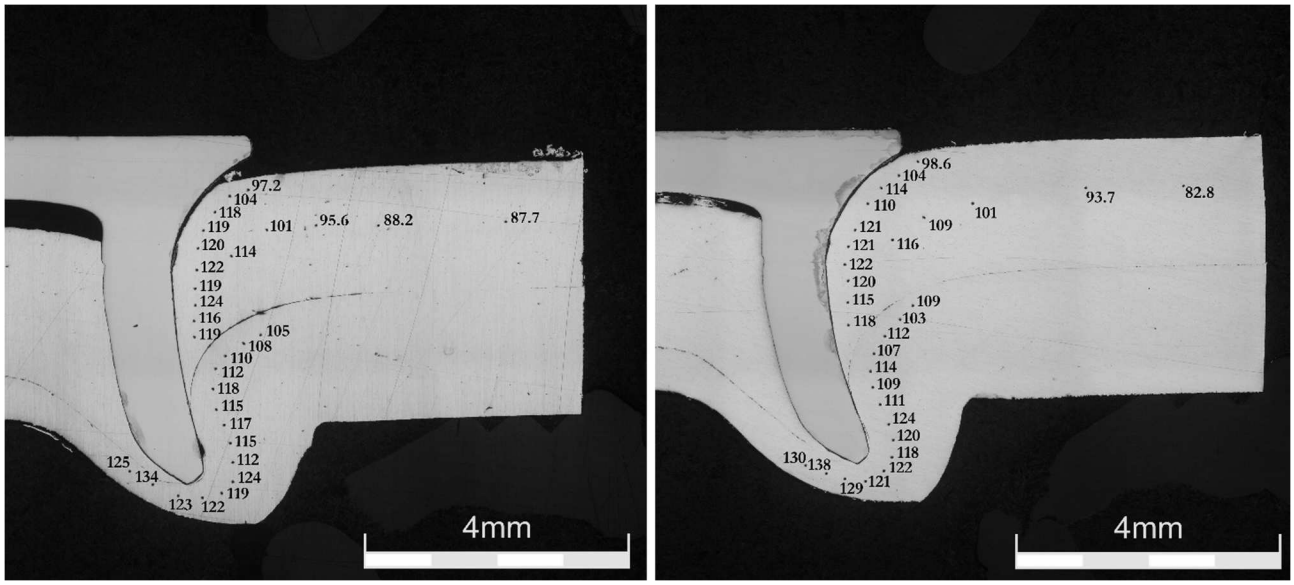

Fig. 7 *Hardness measurement for samples 8 MPa (left) and 10 MPa (right)*

6 Non-contact optical scanning of testing samples to determine flatness

Optical 3D scanner ATOS III TripleScan from German company Carl Zeiss GOM Metrology Gmbh was used for non-contact optical scanning of testing samples. It is a truly professional system, which is nowadays commonly used in many industrial branches e.g. design, control quality, construction and so on. The entire measurement and subsequent processing of scanned data were done in the software GOM ATOS, resp. GOM Inspect Professional, in cooperation with the Technical University of Liberec - Department of manufacturing systems and automation.

As a major result of this optical scanning, there was used flatness evaluation. There was monitored not only the precise value of flatness but also its distribution on the whole testing surface. In Fig. 8 is shown such flatness evaluation for sample 6 MPa. Note, that were always evaluated two planes – plane 1 for the area without the rivet (so no deformation was expected here, and it was the reference plane) and plane 2, which revealed deformation.

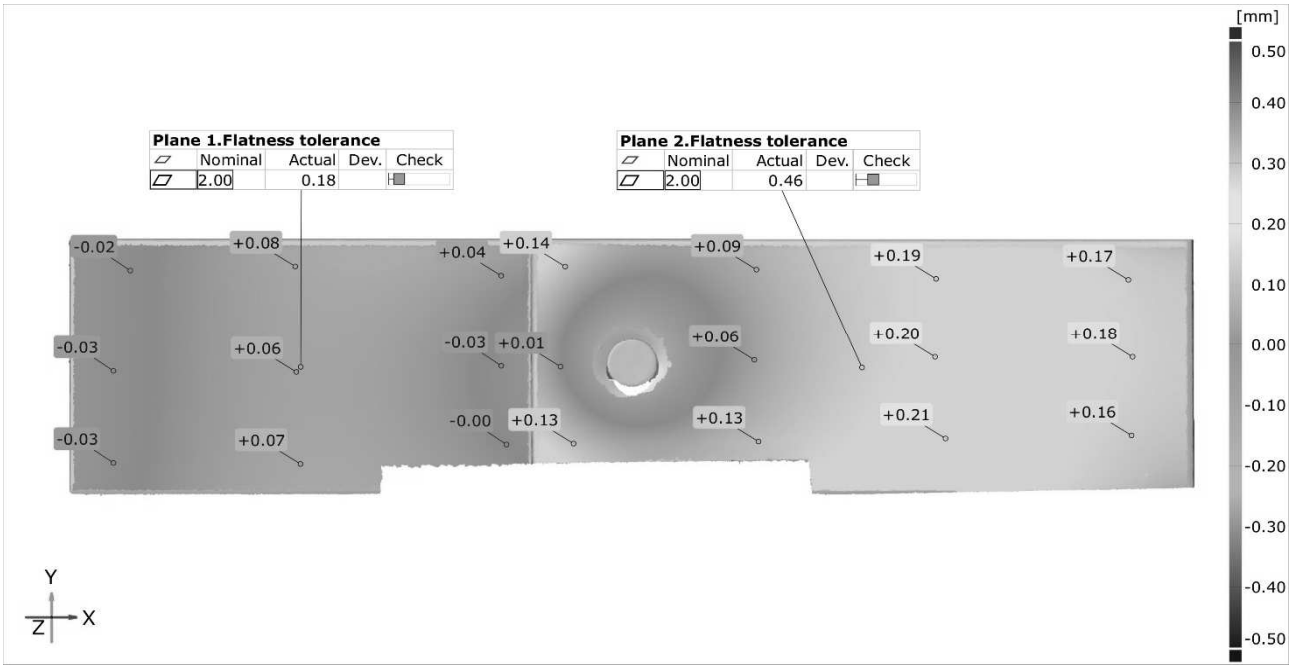

Fig. 8 *Flatness evaluation for sample 6 MPa (front side and including rivet area)*

Moreover, every sample was also scanned from both sides (see Tab. 4) and also with and without the rivet area. Fig. 9 shows such flatness evaluation (without rivet area) for sample 6 MPa, which was taken as the reference one.

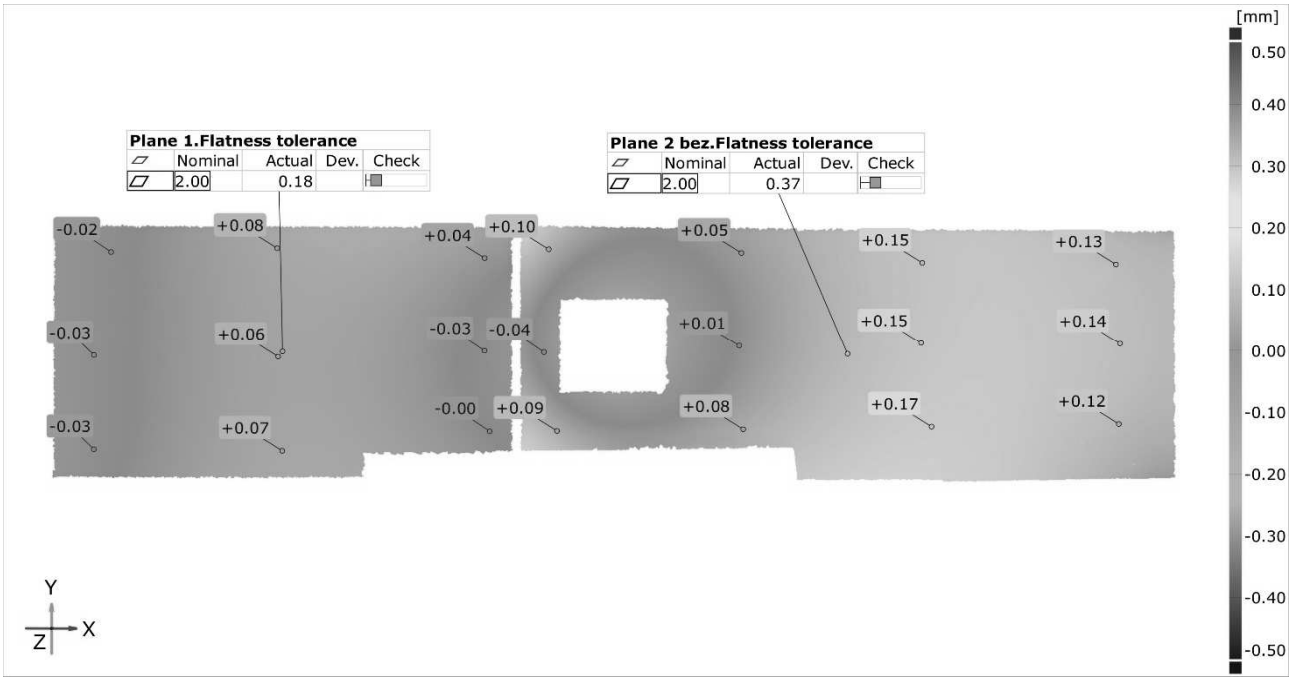

Fig. 9 *Flatness evaluation for sample 6 MPa (front side and excluding rivet area)*

In Fig. 10 is shown the flatness evaluation for the sample 8 MPa. For reasons of space, there is shown only one evaluation image – that one for the front side and including the rivet area. In this position, it is evident that results of the plane 1 are very similar to the previous results (see Fig. 8). On the other hand, it is possible to easily compared deformation in the region of plane 2, which is quite larger (approx. by 21 %) compared to the sample 6 MPa. Other results of the flatness evaluation (back side including rivet area and both sides with/without rivet area) of the sample 8 MPa, which are not graphically shown here, are summarized in Tab. 4.

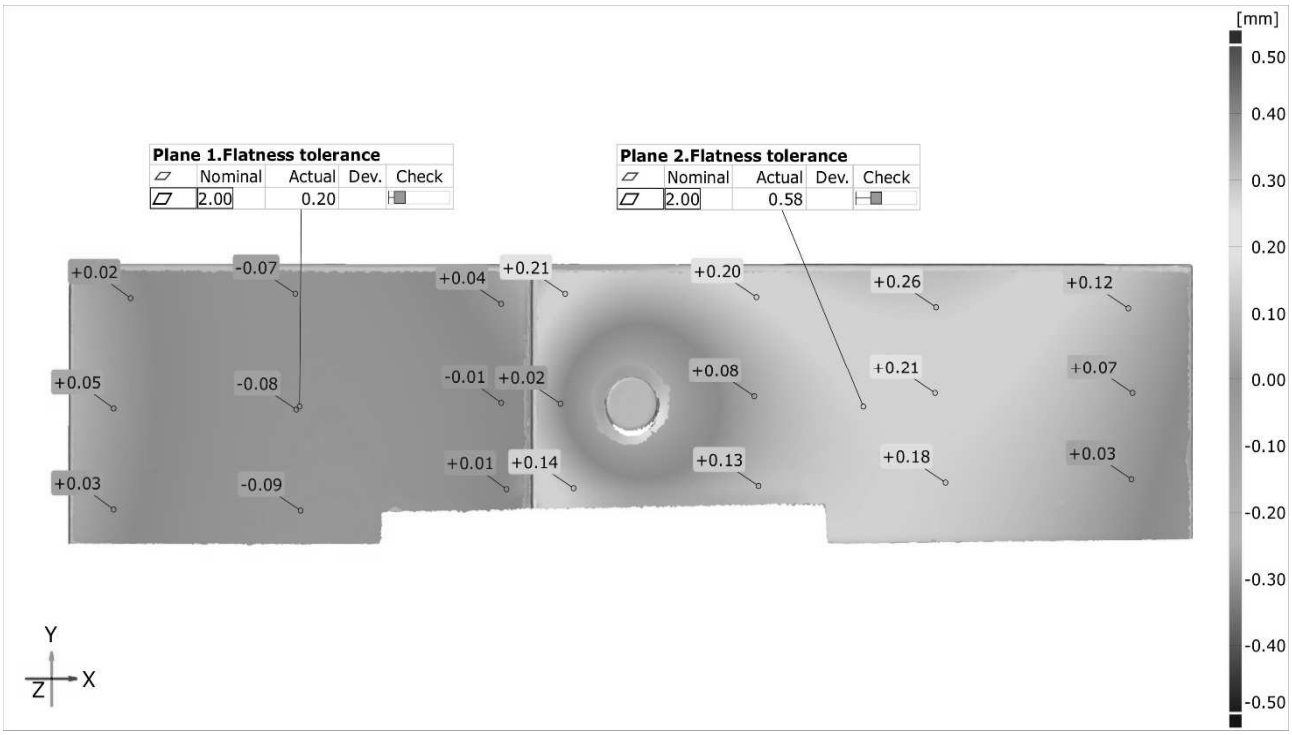

Fig. 10 *Flatness evaluation for sample 8 MPa (front side and including rivet area)*

The same approach was of course used for the sample 10 MPa, where Fig. 11 gives a basic overview of flatness distribution for the front side with rivet area. Again, results of the plane 1 are very similar to the previous cases (6 MPa and 8 MPa), because as this region is without rivet area, there isn´t almost any deformation. However, the flatness evaluation of plane 2 revealed two interesting results. The first one is about quite larger deformation zone about the rivet – compared with the previous ones. The second one rests in the own magnitude of the given flatness (0.82 mm) which is approx. by 78 % higher value than in the case of sample 6 MPa.

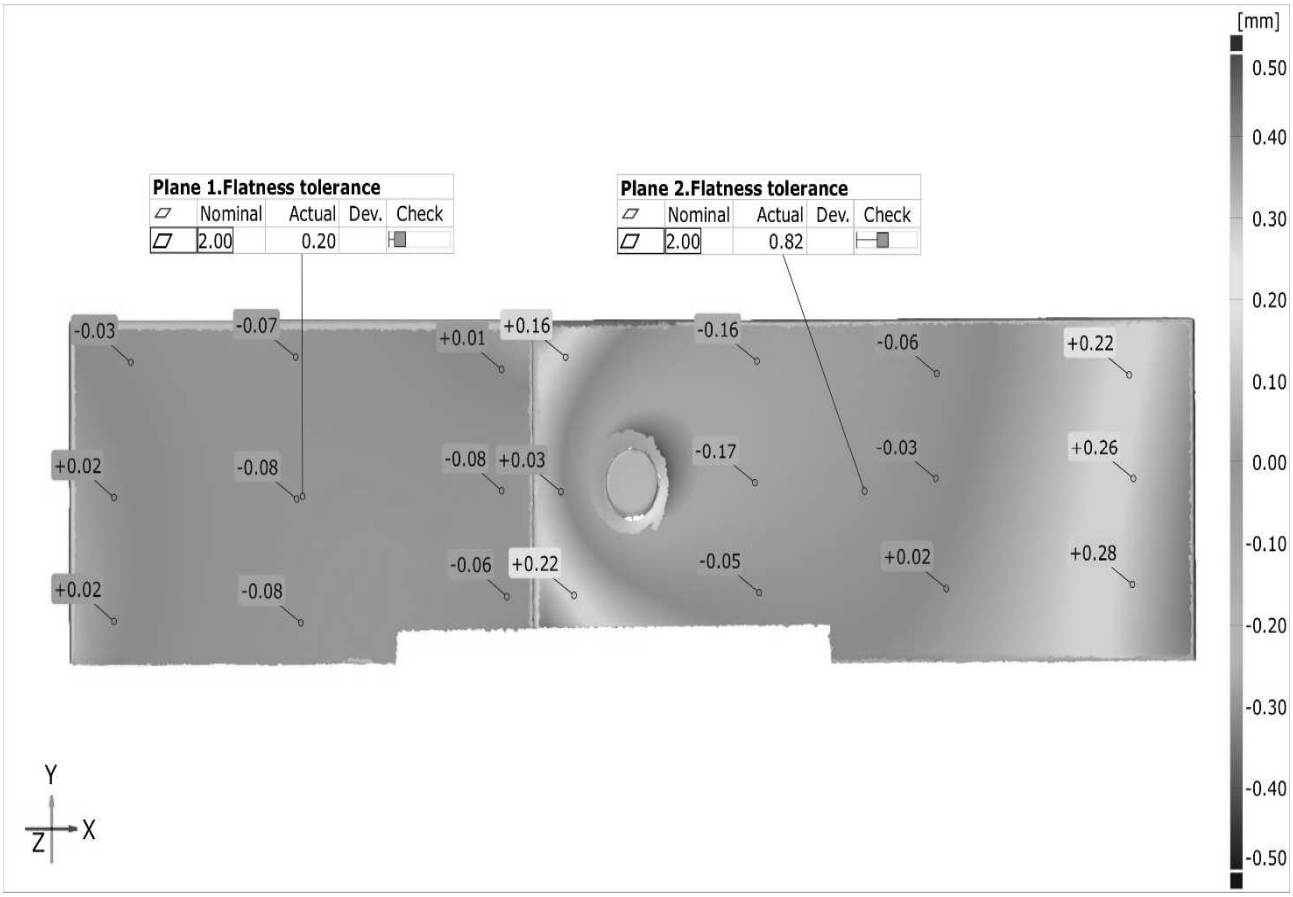

Fig. 11 *Flatness evaluation for sample 10 MPa (front side and including rivet area)*

Flatness evaluation both for plane 1 and plane 2 of all tested pressures (6, 8 and 10 MPa) and for front sides of samples in a graphical illustration is shown in Fig. 12. For every applied pressure are there also shown results not only including rivet area but there is also shown flatness evaluation for samples excluding rivet area. Note that in light of plane 1, there aren´t almost any differences over all tested pressures. All measured results (including both sides of samples as well as flatness evaluation with/without rivet area) are summarized in Tab. 4.

As there was already mentioned before, in Tab. 4 are shown all measured combinations. From the plane 1 point of view, there can be stated that all results are very similar and so there is no influence of riveting force on the flatness of such part. Such reality is of course given by the methodology of measurement, where plane 1 is always taken without influence of the rivet. More interesting results can be observed in the case of plane 2, because such part is already affected by the rivet area. Generally, the higher applied pressure, the higher deformation in light of flatness evaluation and this is valid both for evaluation with/without rivet area and for both sides of samples.

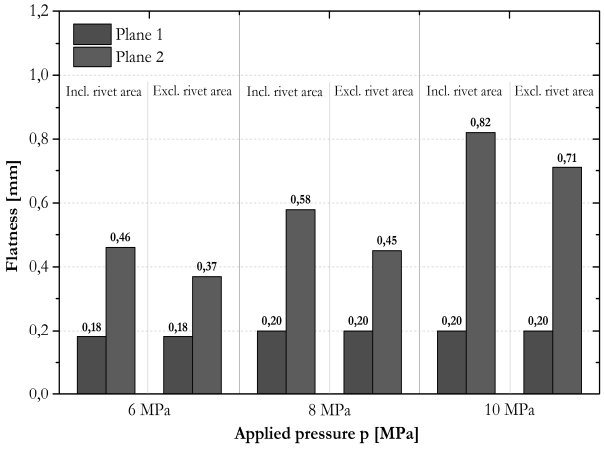

Fig. 12 *Graphical comparison of the flatness evaluation – results for front sides of samples*

Tab. 4 *Final comparison of the flatness evaluation – all tested combinations*

Flatness [mm]		Including rivet area		Excluding rivet area	
		Front side	Back side	Front side	Back side
6 MPa	plane 1	**0.18**	0.19	**0.18**	0.19
	plane 2	**0.46**	0.48	**0.37**	0.33
8 MPa	plane 1	**0.20**	0.24	**0.20**	0.24
	plane 2	**0.58**	0.79	**0.45**	0.66
10 MPa	plane 1	**0.20**	0.20	**0.20**	0.20
	plane 2	**0.82**	0.84	**0.71**	0.70

7 Conclusion

The submitted paper deals with the possibility to provide a basic overview of the deformation behaviour of a given rivet applied for joining aluminium alloy EN AW-6061 (thickness 2 mm). There were used three levels of riveting force (more precisely – pressure) such as following: 36 kN, 48 kN and 60 kN (6 MPa, 8 MPa and 10 MPa). For a final comparison, results from 6 MPa were always taken as the basic ones (so 100 %). After determining the basic mechanical values, two material tests (shear test and hardness testing) as well as one contact-less optical scanning to describe required deformation behaviour, were performed.

The increase of the maximal shear force in dependence on applied pressure was as follows: higher by 15 % for 8 MPa and by 26 % for 10 MPa. Note that the dependence seems not to be linear, but there should be performed more testing levels to confirm such conclusion. Quite time-consuming was the determination of the hardness HV01 distribution along the rivet area. There were determined following maximal hardness HV01 values: 129, 134 and 138, respectively. However, much more important they seem to be distributions of these hardness values because they can be used e.g. in the results from numerical simulation of riveting (via strain distribution).

Deformation analysis was performed with the help of the optical 3D scanner ATOS III TripleScan. As a major result of this experimental procedure, there was evaluated the flatness. Applied pressures and own shape of the testing sample made it possible to evaluate flatness from many different aspects. So, on every sample were always evaluated plane 1 (physically without the rivet) and plane 2 (physically with a rivet). In addition to that, flatness evaluation of plane 2 was performed both with graphically included rivet area and without that area. Finally, there were scanned both sides (front and back) of the testing samples. Thus, there were monitored quite a lot of different combinations in light of flatness evaluation. The most important of them are shown graphically in Chap. 6 and all of them can be found in Tab. 4. Results of all tested planes 1 are very similar because there wasn´t almost any deformation in this part of the testing samples. More interesting results are concerned with planes 2, which are affected by the applied magnitude of riveting force (more precisely - pressure). Generally, the higher riveting force, the higher magnitude of flatness. From the front side point of view, there aren´t significant differences between results including and excluding the rivet area. If there is taken applied pressure 6 MPa as 100 %, flatness evaluation for 8 MPa is higher by 26 % (29 %) and 10 MPa by 78 % (102 %) in light of including and excluding rivet area, respectively. The same trend is obvious also for the back sides. Nevertheless, in this case, can be such results summarized as higher by 64 % (100 %) and 75 % (112%) – again for 8 MPa and 10 MPa.

In addition to a simple evaluation of the riveting force influence on the quality of riveted joints from aluminium alloy EN AW-6061, which results are summarized in the previous chapters, there was also an effort to provide a basic overview of the more general evaluation of the riveting joints. Especially the possibility of subsequent usage of measured data – e.g. in the numerical simulations. That is why there was used also hardness testing and mainly also contact-less optical scanning to describe the deformation along the rivet area. And just the use of these results is the next step for the research described above.

References

[1] BRADÁČ, J., SOBOTKA, J. (2020). Technical and Economic Aspects of Using Magnesium Alloys for Production of Car Components. In: *Proceedings of the 1st International Conference on*

Automotive Industry 2020, ŠKODA AUTO University, pp. 258 – 266, ISBN 978-80-7654-016-3

[2] GIULIANO, G., POLINI, W. (2021). Weight Reduction in an AA2017 Aluminum Alloy Part through the Gas Forming Process of a Blank with a Variable Thickness. In: *Manufacturing Technology*, Vol. 21, No. 2, pp. 192 – 198. ISSN 1213–2489

[3] GODE, C. (2021). Influence of a low-temperature plastic-deformation process on the microstructure of an Al-Si-Mg aluminum alloy. In: *Materiali in Tehnologije / Materials and Technology*, Vol. 55, No. 2, pp. 283 – 291. ISSN 1580–2949

[4] LAH, A. Š., et al. (2021). The Influence of chemical composition and heat treatment on the mechanical properties and workability of the aluminium alloy EN AW 5454. In: *Materiali in Tehnologije / Materials and Technology*, Vol. 55, No. 5, pp. 709 – 716. ISSN 1580–2949

[5] WANG H., YANG, K., LIU, L. (2018). The analysis of welding and riveting hybrid bonding joint of aluminum alloy and polyether-ether-ketone composites. In: *Journal of Manufacturing Processes*, Vol. 36, pp. 301 – 308. ISSN 1526–6125

[6] KALINA, T., SEDLÁČEK, F. (2019). Design and Determination of Strength of Adhesive Bonded Joints. In: *Manufacturing Technology*, Vol. 19, No. 3, pp. 409 – 413. ISSN 1213–2489

[7] AJABSHIR, S. Z., KAZEMINEZHAD, M., KOKABI, A.H. (2021). Manufacturing thinned friction-stir welded 1050 aluminum by post rolling: microstructure and mechanical properties. In: *Materiali in Tehnologije / Materials and Technology*, Vol. 55, No. 5, pp. 609 – 617. ISSN 1580–2949

[8] PAN, B, et al. (2021). Corrosion behavior in aluminum/galvanized steel resistance spot welds and self-piercing riveting joints in salt spray environment. In: *Journal of Manufacturing Processes*, Vol. 70, pp. 608 – 620. ISSN 1526–6125

[9] KASCAK, L., et al. (2020). Mechanical joining of aluminium alloy sheets. In: *MM Science Journal*, No. 5, pp. 4179–4182. ISSN 1805-0476

[10] ZHANG, H. (2020). Influence of riveting sequence/direction on distortion of steel and aluminum sheets. In: *Journal of Manufacturing Processes*, Vol. 53, pp. 304 – 309. ISSN 1526–6125

[11] BĚHAL, J., RŮŽEK, R. (2021). Effect of the rivet-hole tolerance on the stress-severity factor. In: *Materiali in Tehnologije / Materials and Technology*, Vol. 55, No. 2, pp. 237 – 242. ISSN 1580–2949

[12] HUANG, Z. C., al. (2022). Physical property and failure mechanism of self-piercing riveting joints between foam metal sandwich composite aluminum plate and aluminum alloy. In: *Journal of Materials Research and Technology*, Vol. 17, pp. 139 – 149. ISSN 2238–7854

[13] MA, Y, et al. (2021). A Comparative Study of Friction Self-Piercing Riveting and Self-Piercing Riveting of Aluminum Alloy AA5182-O. In: *Engineering*, Vol. 7, pp. 1741 – 1750. ISSN 2095–8099

[14] KARATHANASOPOULOS, N., PANDYA, K. S., MOHR, D. (2021). An experimental and numerical investigation of the role of rivet and die design on the self-piercing riveting joint characteristics of aluminum and steel sheets. In: *Journal of Manufacturing Processes*, Vol. 69, pp. 290 – 302. ISSN 1526–6125